UNIVERSITI
MALAYSIA
KELANTAN

The Effect of Using Different Firing Temperatures of Waste Glass for The Production of Glass Bricks

Tan Yong Jin
J20A0700

A thesis submitted in fulfilment of the requirements for the degree of Bachelor of Applied Science (Materials Technology) with Honours

FACULTY OF BIOENGINEERING AND TECHNOLOGY
UMK

2023

DECLARATION

I declare that this thesis entitled "The Effect of Using Different Firing Temperatures of Waste Glass for The Production of Glass Bricks" is the results of my own research except as cited in the references.

Signature :_____

Student's Name : TAN YONG JIN

Date : _____

Verified by : _____

Signature : _____

Supervisor's Name : DR NORFADHILAH BINTI IBRAHIM

Stamp : _____

Date : _____

ACKNOWLEDGEMENT

First and foremost, I would like to express my deepest appreciation to my supervisor, Dr Norfadhilah Binti Ibrahim who has given me guidance and constant supervision as well as guiding and teaching me regarding to my final year project. Her guidance, monitoring and constant encouragement are very important to the success for this project.

Second, my gratitude also been extended to UMK's lab assistants for helping and guiding me with lab works and characterization machines. I would like to thanks Mrs Hanisah, Mrs Idayu, Mr Qamal, and Mrs Syahida for guiding me with the experiments conducted. Furthermore, I would like to thanks my course mates Sakthy and Tisha who always helping me and teaching me.

Last but not least, I would like to give a profound appreciation to my parents as well as other family members for their support and passion to me in finishing my research even through the time given to complete this project is limited. Without all of this, I might not able to complete this thesis writing properly. At the end, special thanks to all people that involved in completing my thesis.

The Effect of Using Different Firing Temperatures of Waste Glass for The Production of Glass Bricks

ABSTRACT

Glass is a popular and common material used in our daily life because of their properties such as transparency, high compressive strength, chemical resistance and durability. Thus, large amounts of waste glass production are unavoidable. Hence, enhancing the recycling of these resources and using them wisely provide a significant challenge to industry and academia. The purpose of this study was to provide a method for recycling waste glass in the production of glass bricks. To achieve this goal, the complete process, encompassing the production of mould, the production of glass bricks and subsequent testing for glass bricks characterization. The waste glass was used in this research for the production of glass bricks. The firing temperature of the production glass bricks were 850 ℃, 950 ℃ and 8 hours exposure time. The properties of mould samples were investigated using X-Ray Diffraction (XRD), Thermogravimetric Analysis (TGA). The properties of waste glass were investigated using XRD and Fourier Transform Infrared (FTIR). The properties of glass bricks after being fired at 850 ℃ and 950 ℃ were investigated using density and porosity test, compression test, and FTIR. The 950 ℃ of glass bricks resulted in higher value of true density and compressive strength, with the low amount of water absorption and apparent porosity compare to 850 ℃ of glass bricks.

Keywords: Glass, Bricks, true density, apparent porosity, compressive strength

Kesan Penggunaan Suhu Pembakaran Berbeza Kaca Sisa untuk Penghasilan Bata Kaca

ABSTRAK

Kaca adalah bahan yang popular dan biasa digunakan dalam kehidupan seharian kerana sifatnya seperti ketelusan, kekuatan mampatan tinggi, rintangan kimia dan tahan lama. Oleh itu, jumlah yang besar sisa kaca tidak dapat dielakkan. Seterusnya, mementingkan kitar semula sumber ini dan menggunakan dengan bijak memberikan cabaran besar kepada industri dan akademik. Tujuan kajian ini adalah untuk menyediakan kaedah untuk mengitar semula sisa kaca dalam penghasilan batu bata kaca. Untuk mencapai matlamat ini, process lengkap untuk kajian ini termasuk pengeluaran acuan, pengeluaran bata kaca dan ujian seterusnya untuk pencirian bata kaca telah dilaporkan. Sisa kaca digunakan dalam kajian ini untuk penghasilan batu bata kaca. Suhu pembakaran untuk batu bata kaca ialah 850 ℃ dan 950 ℃ dengan masa pendedahan ialah 8 jam. Sifat sampel acuan telah dikenal pasti menggunakan “X-Ray Diffraction (XRD)” and “Thermogravimetric Analysis (TGA)”. Selain itu, sifat sisa kaca telah dikenal pasti menggunakan XRD dan “Fourier Transform Infrared (FTIR)”. Sifat batu bata kaca selepas dibakar pada suhu 850 ℃ dan 950 ℃ telah dikenal pasti menggunakan ketumpatan, keliangan, kekuatan mampatan dan FTIR. 950 ℃ suhu batu bata kaca menghasilkan nilai ketumpatan dan kekuatan mampatan yang lebih tinggi dan kadar penyerapan air dan keliangan yang lebih rendah berbanding dengan 850 ℃ suhu batu bata.

Kata kunci: Kaca, batu bata, ketumpatan, ketara keliangan, kekuatan mampatan

TABLE OF CONTENTS

LIST OF TABLES

LIST OF FIGURES

LIST OF ABBREVIATIONS

SiO_2	Silicon Dioxide
Na_2O	Sodium Oxide
CaO	Calcium Oxide
XRD	X-ray Diffraction
XRF	X-ray Fluorescence
OM	Optical Microscope
$CaSO_4 \cdot 2H_2O$	Plaster of Paris
FTIR	Fourier Transform Infrared Spectroscopy
SEM	Scanning Electron Microscope
CMM	Clay Mix Mould

LIST OF SYMBOLS

±	Plus-minus
%	Percentage
wt.%	Weight percentage
MPa	Megapascal
g/cm^3	Gram per cubic centimetre
ºC	Degree Celsius
Psi	Pound-force per square inch
cm	Centimeter
ºC/m	Degree Celsius per minute
μm	Micrometer
mm	Millimetre
θ	Theta
º	Diffraction angle
s	Second
kN	Kilovolt
MPa/s	Megapascal per second
cm^{-1}	Reciprocal centimeter (wavenumber)

CHAPTER 1

INTRODUCTION

1.1 Background of Study

As all of us know, glass is a famous, popular and basic material. Glass is an inorganic solid, transparent, brittle, hard and durable material. The application of glass is many and we used it in our daily life (Achintha, 2016). For example, it is use in construction, packaging, application of electronics and medical field. Besides that, there are many types of glass such as the most common glass are silicate glass and soda-lime silica glass. The products of soda-lime silica glass are windows, lightbulb and bottles. Silicon dioxide is a main material for the production of silicate glass. On the other hand, silicon dioxide (SiO_2), sodium oxide (Na_2O) and calcium oxide (CaO) are the raw materials for the production of soda-lime glass (Hamidon et al., 2015). Next, the examples for the glass that are used in construction are float glass, shatterproof glass, laminated glass, tinted glass and the rest. The properties of glass are heat resistance, chemical resistance and pressure resistance (Achintha, 2016).

Nowadays, glass has too many applications and the number of the production of glass is too huge, lead to the waste glass increase inevitable. In Hong Kong, the total amount of waste glass generated annually is 64,000 tons, but only 8,000 tons are recycled (Chen et al., 2002). In addition, glass is a non-biodegradable material and it takes up to four thousand years to decompose in the environment. Next, the waste glass requires a big valuable space to become a landfill and lack of the land to fill the waste

glass is a new challenge. Then, landfill may cause serious environmental problems. For example, soil pollution and water pollution.

The solid waste generation in Malaysia has increase from 39 tonnes per day in 2015 to 50 tonnes per day in 2020. The waste glass in Johor is 92 ± 71 tonnes per year, Kuala Lumper is 44 ± 16 tonnes per year and Negeri Sembilan is 24 ± 23 tonnes per year. In 2020, the recycled rate in Malaysia is increase from 10.5% in 2012 to 22% in 2020. However, the recycled rate is insufficient to decrease the rate of landfill for waste glass (Rangga et al., 2022). Thus, the number of recycled waste glass need to increase and the number of landfills need to decrease.

Apart from that, glass brick is a significant transparent construction material. The glass bricks applied for the first time in 1914 by architect Bruno Taut in his famous glass house on the occasion of an exhibition in Germany. Glass bricks can be produced in the desired shape and size for aesthetic application. Generally, the chemical composition of glass bricks are SiO_2 and Na_2O. The advantages of glass bricks are high thermal resistance, transmit of light, and good mechanical properties (de Moraes et al., 2008). In previous study, the researchers have produced the hollow glass bricks by using 100% wt. of waste glass (Brito et al., 2023).

In this research will use waste glass for production of glass bricks. Furthermore, the structure and the morphology of the glass bricks of waste glass will study by using visual inspection. The other test will undergo are density and porosity test, compressive test, XRD, FTIR and TGA.

1.2 Problem Statement

Glass is a famous and common material due to their transparency, durability, chemical resistance and aesthetic appeal. The application of glass can be used in many

fields. For instance, using glass on packaging such as bottles for drinks and tableware which is drinking glasses, plates and bowls. Next, glass is often used on housing and building field. Example of a product is windows (Achintha, 2016). Besides that, the application of glass in the medical field is photographic slides, microscopic glasses and the list goes on. Glass can be used in various applications with different functions.

However, glass has become a serious environmental problem all over the world because glass is a non-biodegradable material (Mehta & Ashish, 2020). It takes up to 4 thousand years to decompose in the environment. On the other hand, some of the type of glass contain some heavy metal or chemical that will harm to the environment. Thus, these waste glass require an enormous amount of landfill area and permanently use the valuable area. Then, this will lead to soil and water pollution occur. The lack of landfill area is a problem will we face in the future. In previous study, using 2% and 4% of waste glass in production of glass bricks didn't show the crucial enhancement in the properties of the bricks (Hasan et al., 2021). The result of the previous study shows the compressive strength of the bricks that contain addition 2% and 4% of waste glass production is increase from 17 MPa to 18 MPa (Hasan et al., 2021). The water absorption is decrease from 14.9% to 14.7% and the density is increase from 1.7 g/cm^3 to 1.8 g/cm^3. Hence, the properties of the bricks improved obviously when the composition of the waste glass increased (Hasan et al., 2021). Thus, the composition of waste glass was used at 100 wt. % in the study to improve the properties of glass bricks obviously and solve the environment problem.

1.3 Objectives

The objectives of this study are:

i. To prepare glass bricks by using waste glass

ii. To identify the suitable firing temperatures for the production of glass bricks

iii. To determine the highest compressive strength of the sample.

iv. To study the suitable mould for the production of glass bricks.

1.4 Scope of Study

The raw material of glass bricks is waste glass. The composition of glass bricks is 100 wt. % of waste glass. Next, the raw materials of POP mould are plaster of paris as a binder, kaolin as a modifier, river sand as a refractory and water. The compositions 1 are 32.5 wt.% of plaster of paris, the wt.% of kaolin is 10 wt.%, the wt.% of river sand is 32.5 wt.% and the wt. % of water is 25 wt.%. The compositions 2 are 57 wt.% of plaster of paris, 10 wt.% of kaolin, 10 wt.% of riversand and 23 wt.% of waters. The composition 3 are 65 wt.% of plaster of paris, 10 wt.% of kaolin, and 25 wt.% of waters.

The second material for production mould is industrial clay and the third composition for production clay mix mould is using ball clay, sawdust and kaolin. The weight percentage of ball clay is 72.5%, 25 wt.% of kaolin, 2.5 wt.% of sawdust and 60mL water.

On the other hand, the parameter used in this study is firing period. This study had 8 samples of glass bricks with two temperatures and 8 hours durations of firing process. The temperatures used in the firing process are 850 ºC and 950 ºC. The reason for using these parameters is high temperature and high exposure time can improve the adhesion of the glass particle and higher true density and increase in compression strength.

1.5 Significances of Study

The properties of glass bricks were extremely crucial for any application because a bad quality of bricks would cause accidents. Thus, the properties of glass bricks of waste glass are required to study. The properties of glass bricks of waste glass need to be the same or surpass with the normal bricks. A normal brick with the suitable water absorption can prevent the brick damage by freezing (Stryszewska & Kańka, 2019). Thus, it is vital to ensure the glass bricks of waste glass can withstand any kind of weather.

In this research, the compressive strength of the glass bricks of waste glass is reached or exceeded with the normal bricks. Next, the compressive strength of glass bricks made from waste glass enhanced. The compressive strength is an extremely important properties for glass bricks because compressive strength can decide the suitability of load-bearing stones for building and avoid the glass bricks of waste glass damaged by the stress.

CHAPTER 2

LITERATURE REVIEW

2.1 Bricks

Admittedly, nowadays it is common that bricks are an extremely significant material for construction for thousands of years. The raw materials of bricks are cement, sand, gravel and water. Based on some research, it has been shown that using fire in the production of bricks yields better performance. Table 2.1 shows the firing cycle process contain six phases (Zhang et al., 2018):

Table 2.1: The phases for firing bricks cycle process

No.	Phase	Temperature (°C)
1	Evaporation (remove moisture)	20-150
2	Dehydration (remove / decompose carbonaceous substances)	149-650
3	Oxidation (burn the carbonaceous remnants)	300-982
4	Vitrification (transform, enhance the strength of bricks)	900-1316
5	Flashing (colour of bricks)	1150-1316
6	Cooling	1316-20

As all of us know, the bricks are hard, durable, fire resistance and superior compressive strength. Normally, the compressive strength of bricks is around 6.865MPa to 10.298

MPa. The water absorption of bricks cannot be more than 12% because it can be damaged by freezing (Stryszewska & Kańka, 2019). However, the compressive strength and water absorption are based on the raw material used. Furthermore, the researcher used municipal waste for production of bricks in previous study. The municipal waste used for production of bricks in previous study are plastic waste, glass waste and other municipal waste (Zhang et al., 2018). Most of the research are using waste glass for the production of bricks because waste glass is suitable for production of the bricks and waste glass contain can help the bricks enhance the compressive strength (MPa) and decrease the water absorption (wt. %) (Demir, 2009). Figure 2.1 shows the normal bricks.

Figure 2.1: Bricks (Source:(Stryszewska & Kańka, 2019))

2.2 Type of Glass

In industrial revolution 4.0, glass have various type such as, soda-lime silica glass, borosilicate glass and lead crystal glass. Borosilicate glass also called as pyrex glass because the raw material of borosilicate glass are barium silicate and sodium silicate. Generally, the application of borosilicate glass is producing laboratory apparatus, lamp and tube envelops. The chemical compositions of borosilicate glass are 70-80 wt.% of silica (SiO_2), 7-13 wt.% of boron oxide(B_2O_3), 4-8 wt.% of sodium oxide (NaO_2) and 2-8 wt.% Aluminium Oxide (Al_2O_3). Next, the chemical compositions of lead crystal glass are 55-65 wt.% of silica(SiO_2), 18-36 wt.% of lead oxide (PbO), 13-15

wt.% of sodium oxide (NaO_2) (Hasanuzzaman et al., 2016). Soda-lime silica glass is a very common and popular type of the glass. The application of soda-lime silica glass are production of bottles and windows because soda-lime silica glass is low cost and has no toxicity. Due to the soda-lime silica glass is transparent and low melting point, thus it is very suitable for production of windows. Typically, the compositions of soda-lime silica glass are 70-75 wt.% of silica (SiO_2), 12-16 wt.% of soda [Sodium Oxide (NaO_2)], 10-15 wt.% of lime [Calcium Oxide (CaO)] and another additive (Hasanuzzaman et al., 2016). The waste glass is extremely suitable for production bricks because it is soda-lime silica glass. From the other research shows soda lime silica glass can improve the properties of bricks such as compressive strength and decrease the water absorption of bricks (Islam et al., 2016).

2.3 Firing Temperature

As all of us know, the glass material can withstand high temperatures because it usually contains soda-lime or silica as thermal resistance material. Thus, the melting point of soda-lime silica glass is between 1400 °C and 1600 °C. The melting point of the glass depends on the composition of the glass. The annealing temperature of soda-lime silica glass is 548 °C and the soda-lime silica glass will start soften and adhesive when temperature reach 700 °C. (Shelby, 2020). In previous study, the firing temperatures apply on sample are 850 °C, 950 °C and 1050 °C (Demir, 2009). Hence the result shows the compressive strength of the sample improves from 18.75 MPa (850 °C) to 24.50 MPa (1050 °C). On the other hand, the water absorption decreases due to the temperature increase from 850 °C to 1050 °C. The water absorption of the sample is decrease from 32.02 wt. % to 12.86 wt. % (Demir, 2009). Thus, have two different temperatures (850 °C and 950 °C) with 8 hours for firing process in this study because

high temperature and high exposure time can enhance the properties of the glass. For example, adhesion of the glass particle, compressive strength and the crystallinity (Brito et al., 2023).

2.4 Characterization Technique

2.4.1 Visual Inspection

Visual inspection is a simple and easy method to detect the defects by using naked eyes to make sure the samples present in a good condition. Nowadays, visual inspection was used some electronic devices such as smart phone and high-quality camera. In this research, smart phone were used to undergo visual inspection of glass bricks to observe the melting level of glass bricks and the surface of glass bricks. Normally, the visual inspection of bricks is used to observe the colour change of bricks with changes in temperature and surface of bricks (Alabduljabbar et al., 2021).

2.4.2 X-Ray Diffraction (XRD)

X-ray diffraction is a good technique used to study the crystal structure of materials, phase identification and show information on unit cell dimensions. XRD is based on the principle of Bragg's law, which states that when X-rays interact with a crystal, they were diffracted at specific angles, depending on the spacing between the atoms in the crystal lattice. By measuring the diffraction pattern of a sample, it is possible to determine the crystal structure of the material, including the arrangement of atoms, the lattice spacing, and the size and shape of the crystal domains. XRD can be used to identify unknown material and study changes in the crystal structure of a material as a function of temperature, pressure, or other conditions. XRD widely used in

scientific research and industrial application (Epp, 2016). The XRD patterns of bricks show in Figure 2.2 and the XRD pattern of waste soda-lime glass present in Figure 2.3.

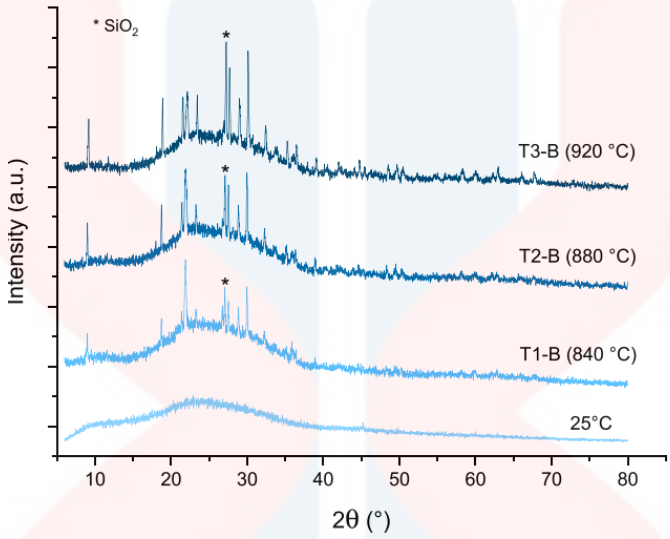

Figure 2.2: XRD patterns of bricks (Source: (Brito et al., 2023))

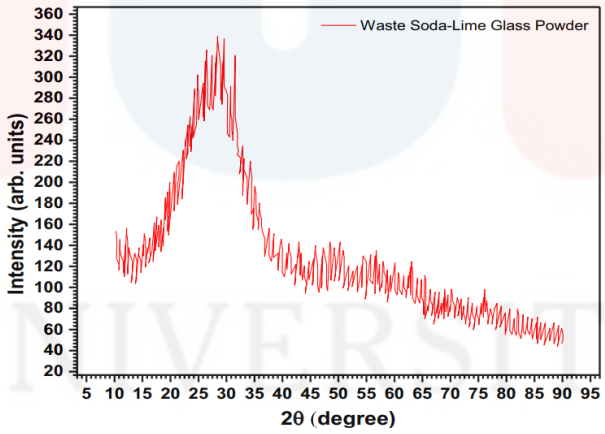

Figure 2.3: XRD pattern of waste soda-lime glass powder (Source: (Hasan et al., 2021))

2.4.3 Thermogravimetric Analysis (TGA)

Thermogravimetric Analysis (TGA) is a common technique for material characterization. TGA can used to measure the weight loss of the sample and heat stability of sample during thermal change. Generally, thermogravimetric analysis used

for reduction, absorption, desorption, decomposition and oxidation (Saadatkhah et al., 2020).

Besides that, the x-axis of the graph for TGA basically is stand for weight or weight (%) and y-axis of the graph for TGA is stand for temperature ℃.

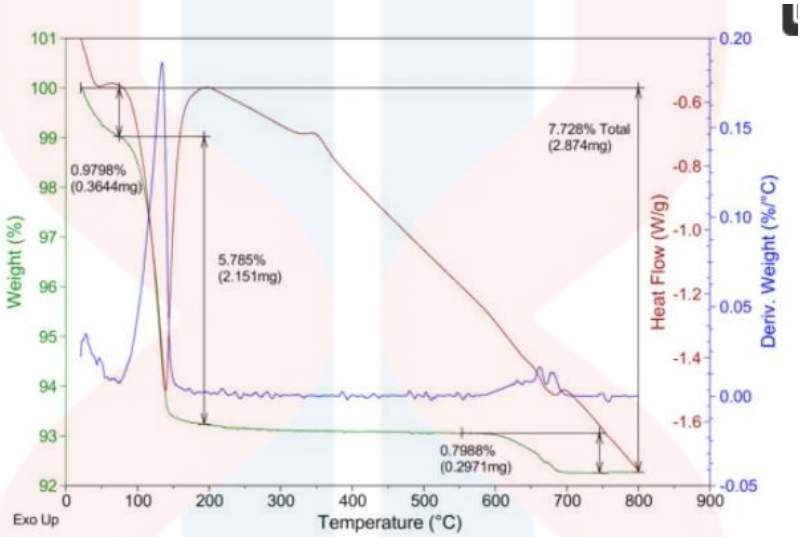

Figure 2.4: The results of thermogravimetric Analysis (TGA) of plaster sample (Source: (Álvarez et al., 2021))

From previous research, the plaster sample conduct the thermogravimetric analysis and the result shows in Figure 2.4 (Álvarez et al., 2021). Based on Figure 2.4, the result shows the weight loss of sample is 0.978% when temperature below 80℃ because of the raw material's physically bonded water being lost. After that, the 5.785% of weight loss occur from the temperature 75℃ to 180℃ because of the dehydration of plaster. When the temperatures reach 550℃ to 700℃, the sample shows the 0.8% of weight loss. The transition phase for plaster sample from soluble to insoluble anhydrite (Álvarez et al., 2021).

2.4.4 Density and Porosity Test

To perform the density test for bricks, a sample of the brick is taken and its mass is measured using a balance. The volume of the brick can be determined by measuring its dimensions, such as length, width, and height, and calculating its volume using appropriate formulas. Alternatively, the volume can be determined by immersing the brick in water and measuring the volume of water displaced by the brick. Once the mass and volume of the brick have been determined, the true density can be calculated by dividing the mass by the volume. The result of the calculation is the true density of the brick. The true density of a brick is an important property that affects its thermal insulation, sound insulation, and load-bearing capacity. Bricks with higher true density are generally stronger and more durable, but they may also be less insulating and heavier than bricks with lower true density. In previous study by Hasan et al (2021), the bulk density of bricks with 40% waste glass decreases by up to 15.5% in Figure 2.5 because carbon dioxide generates in the bricks.

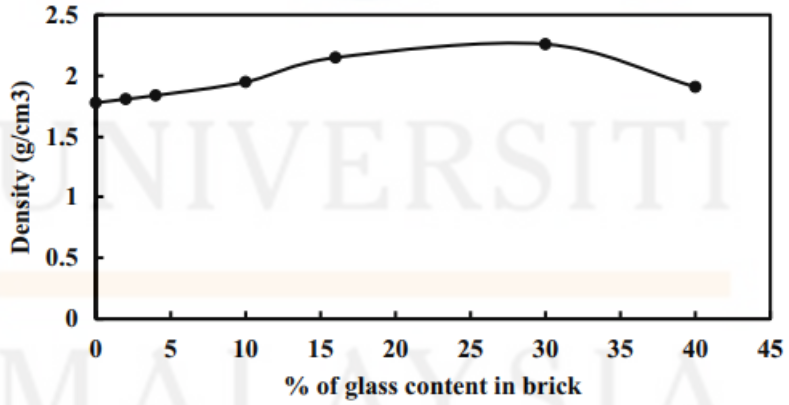

Figure 2.5: Density of the bricks (Source: (Hasan et al., 2021))

The porosity test for bricks is a procedure used to determine the porosity of a brick, which is a measure of the volume of open spaces, or pores, within the brick. Bricks with high apparent porosity are generally less strong and less durable than those

with low apparent porosity. In Figure 2.6 show increase the composition of waste glass can decrease the apparent porosity of the bricks (Hasan et al., 2021).

Water absorption of bricks refers to the amount of water that is absorbed by the bricks when they are immersed in water for a certain period of time. It is an important property of bricks that affects their durability, strength, and overall performance. Water absorption is usually expressed as a percentage of the weight of the dry brick. The test involves soaking the brick in water for a specified period of time, typically 24 hours, and then measuring the weight of the brick before and after soaking. The difference in weight is used to calculate the water absorption percentage. The water absorption of bricks is influenced by a variety of factors, including the apparent porosity of the brick, the size and distribution of the pores, and the density of the brick. Bricks with high water absorption are more susceptible to damage from freezing and thawing cycles, as well as from exposure to moisture and humidity over time. They may also be more prone to efflorescence, which is the formation of white salt deposits on the surface of the brick due to the movement of moisture through the material. Normally, the water absorption of bricks is below than 10%. The result of water absorption is decrease from 15.25% to 5.62% for the bricks with 40% waste glass in Figure 2.6 (Hasan et al., 2021).

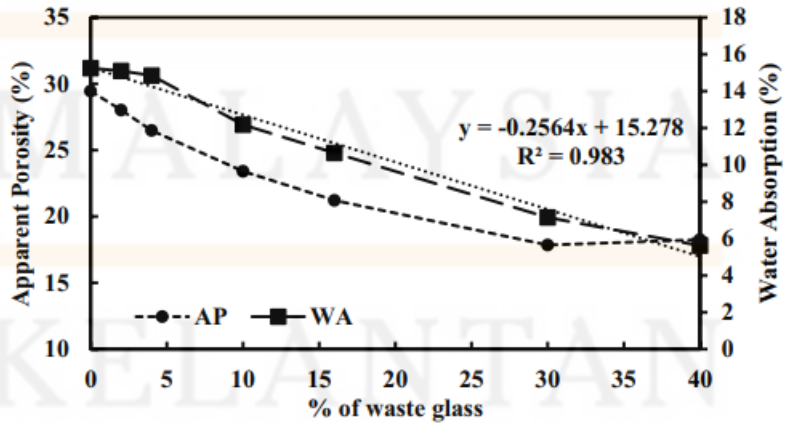

Figure 2.6: Apparent porosity and water absorption (Sources: (Hasan et al., 2021))

2.4.5 Compression Test

The compression test of bricks is a procedure to determine the compressive strength of the bricks. The compression test can be defined by the amount of force a sample can withstand. The test involves applying a compressive load to a sample of the brick until failure occurs. The load at which the brick fails is recorded and used to calculate the compressive strength of the brick (Aubert et al., 2016). In previous research by Hasan et al (2021), the apparent porosity of the bricks decreases, the compressive strength of the bricks will increase. Figure 2.7 present the relationship between apparent porosity and compressive strength.

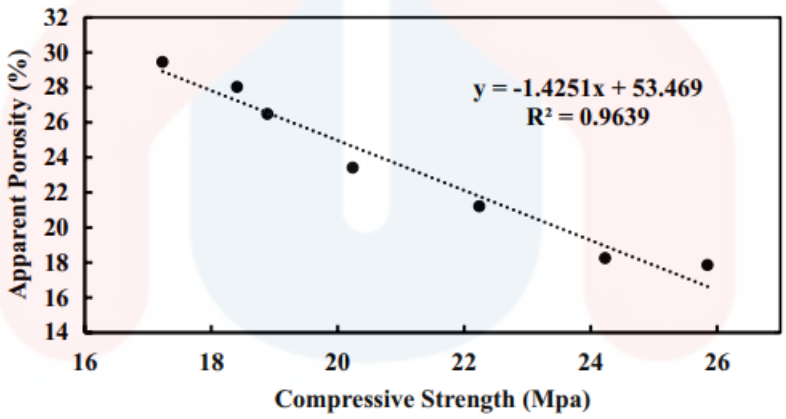

Figure 2.7: The result of compressive strength (Source: (Hasan et al., 2021))

2.4.6 Fourier Transform Infrared (FTIR)

Fourier transform infrared (FTIR) spectroscopy is a unique characterization technique to identify the chemical compound, functional group present in organic and inorganic compound by measuring their absorption by measuring their absorption of infrared radiation over a range of wavelengths. Besides that, FTIR can used to observe the local structure of silicate glasses, which allows one to determine changes on the Si-

O-Si vibrational modes. Figure 2.8 show the FTIR spectra of soda lime silica. Based on previous report, there are three primary absorption bands in the FTIR absorption spectra such as 470 cm^{-1} attributed to Si-O-Si bending vibration, 780 cm^{-1} attributed to Si-O-Si symmetric stretching and 1050 cm^{-1} attributed to Si-O-Si asymmetric stretching.

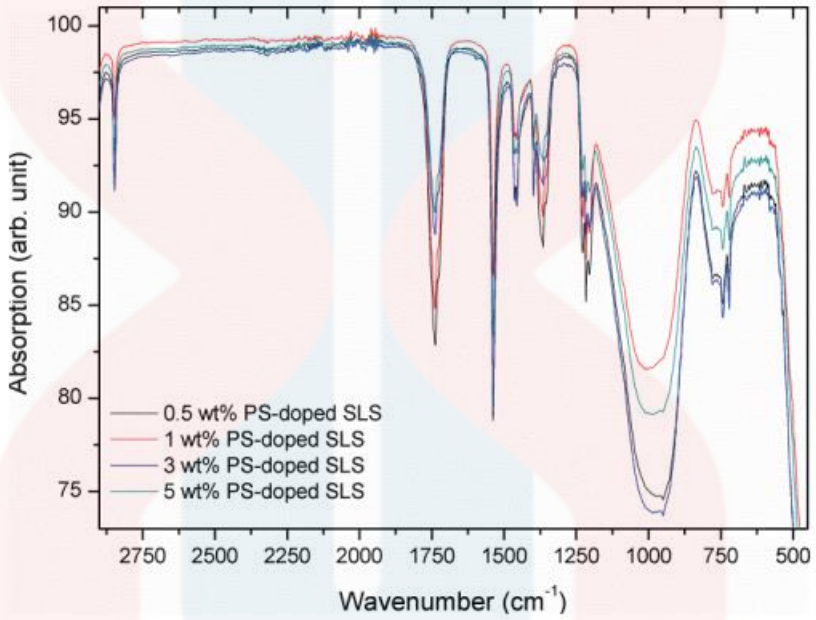

Figure 2.8: The FTIR spectra of the Soda lime silica sample (Source:(Aktas et al., 2016))

CHAPTER 3

MATERIALS AND METHODS

3.1 Materials

The brick is made of waste glass which is soda-lime silicate. In this study, the bricks of a waste glass sample were prepared by using soda-lime silicate waste glass. The difference firing temperature and same exposure time in the furnace were applied for the sample as shown in Table 3.1. The properties of the bricks of waste glass samples were identified by using some characterization method. For example, compressive test and water absorption test. The composition of bricks is prepared 100 wt. % of the colourless waste glass.

Table 3.1: The composition of raw materials and firing temperature & time

100 wt.% of Waste Glass				
Temperature ℃	8 Hours Exposure Time (8 sample)			
850	850(1)	850(2)	850(3)	850(4)
950	950(1)	950(2)	950(3)	950(4)

3.2 Sample Preparation

3.2.1 Crushing

The waste glass crushed into small pieces. The particle size of the waste glass might be between 0.2 cm and 0.5 cm**.** It is because the very fine particle size of the waste glass was detrimental to human health.

3.2.2 Sieving

The cullet of waste glass was sieved through 0.2 cm to 0.5 cm. This is because to ensure the cullet didn't contain any residue. The residue may affect the properties of the bricks such as the compressive strength, apparent porosity and true density. In this study was used test sieve to sieve the cullet of waste glass. After the sieving process, the cullet of waste glass was fill into the mould.

3.2.3 Firing

The three different temperatures and three different exposure times to firing the sample. From Table 3.1, the samples were fired at 850 ℃, 950 ℃ with 8 hours of firing period.

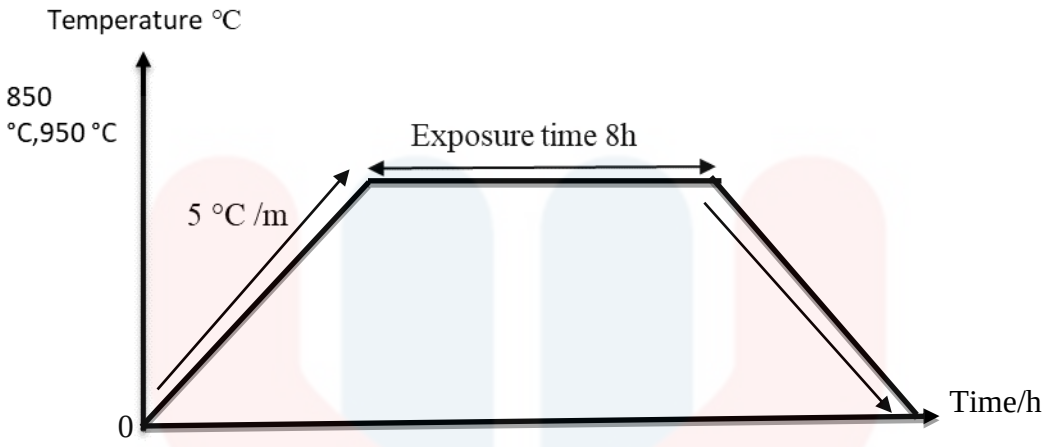

Figure 3.1: Graph of bricks firing process

3.3 Mould Preparation

3.3.1 Raw Material

The raw materials of the mould were separate with 3 important types of material which are binder, modifier and refractory. In this study was used gypsum plaster as a binder, kaolin as a modifier and river sand as a refractory. The chemical composition of plaster of paris is ($CaSO_4 \cdot 2H_2O$). It acts as a binder because it is a material that can set and harden quickly (Brito et al., 2023). Besides that, kaolin is very common as a modifier because of it has low surface changes, high fusion point and it remains stable in size after absorbing water and does not expand (Zheng et al., 2023). After the plaster binder has lost its crucial strength, the refractory provides stability to the mould. Last, water is an important material for mould. Based on Table 3.2, the first composition of POP mould 1 contained 32.5 wt.% of plaster of paris, 10 wt.% of kaolin, 32.5 wt.% of river sand and 15 wt.% of water. The second composition of pop mould 2 contained 57 wt.% of plaster of paris, 10 wt.% of kaolin, 10wt.% of river sand, 23 wt.% of water in Table 3.3. From Table 3.4 shows the third composition of pop mould 3 contained 65 wt.% of plaster of paris, 10 wt.% of kaolin, 25 wt.% of water.

Table 3.2: The composition of POP mould 1

Raw Material	Weight Percentage (wt.%)
Plaster of Paris	32.5
Kaolin	10
River Sand	32.5
Water	15

Table 3.3: The composition of POP mould 2

Raw Material	Weight Percentage (wt.%)
Plaster of Paris	57
Kaolin	10
River Sand	10
Water	23

Table 3.4: The composition of POP mould 3

Raw Material	Weight Percentage (wt.%)
Plaster of Paris	65
Kaolin	10
Water	25

Based on Figure 3.2, the industrial clay was used for the production clay mould. After that, the raw materials of clay mix mould were ball clay with 72.5 wt.%, kaolin with 25 wt.% and sawdust with 2.5 wt.% from Table 3.5. This composition was mixed with 60mL water for the production of clay mix mould.

Figure 3.2: Industrial Clay

Table 3.5: The composition of clay mix mould

Raw Material	Weight Percentage (wt. %)
Ball Clay	72.5
Kaolin	25
Sawdust	2.5

3.3.2 Sieving

To remove the contaminants and larger grain, the sand used in the mould passed through a mesh size between 0.3 mm to 0.7 mm.

3.3.3 Mixing

The raw materials of POP mould (Plaster of Paris, kaolin and river sand) were mixed together and stirred properly. After that, the water was added into the mixture, stirred properly again and ensure all the raw material was mixed together. The raw materials of clay mix mould (Ball clay, kaolin, sawdust) were mixed together and stirred properly. The water was added into the mixture of raw material and stirred properly again.

3.3.4 Drying

The POP mould, industrial clay mould, clay mix mould were dried at room temperature for 5 days. After 5 days, POP mould, industrial clay mould, clay mix mould were dried in oven with 100℃ for 1 day. After the drying process in oven, POP mould, industrial clay mould, clay mix mould were undergo firing process with 750℃ for 6 hours.

3.4 Sample Characterization

3.4.1 Visual Inspection

In this study, visual inspection was used to study the surface and inner appearance of the glass bricks after melting by using smart phone to capture the image.

3.4.2 X-Ray Diffraction (XRD)

In this study, x-ray diffraction used to study the crystal structure of material and phase of a material as well as to measure the intensity and position of the diffraction peaks. Thus, the crystalline peak and intensity of peaks could be studied from x-ray diffraction (XRD). The diffraction patterns were captured at a scan rate of 2 º/min with 2θ, ranging from 10 º to 90 º. All of the sample require to sieve through 0.074 mm mesh size. The machine used in XRD testing was the Bruker D2 Phaser.

3.4.3 Density and Porosity

The density test determined the true density of compacted materials. It involves measuring the mass and volume of the compacted material and then calculating the true

density by dividing the mass by the volume. The porosity test was used to study the size of the pores in the bricks because the size of the pores might affect the properties of the glass bricks. Water absorption was performed to assess their durability, including the degree of burning, quality and behaviour of the bricks in response to weathering. Water absorption was measured by the vacuum. The air was evacuated by using a glass desiccator and the sample was immersed in water. Thus, the weights before and after the sample was immersed in water were measured, and the water absorption was calculated by using equation 3.1. True Density and apparent porosity were conducted by using densimeter and calculated by using equation 3.2 and equation 3.3. The calculation formula referred to MS ISO 10545-3:2001. The equation:

Water absorption equation: Equation 3.1

$$W.A = \frac{w_o - w}{w_o} \times 100\%$$

True Density equation: Equation 3.2

$$P = \frac{m}{v}$$

P = density

m = mass

v = volume

Apparent Porosity equation: Equation 3.3

$$p = \frac{m2_v - m1}{m1} \times 100$$

$$V = m2_v - m3 \times 100$$

3.4.4 Compressive Test

The compression test was used to determine the stress of glass bricks can withstand by using Universal Testing Machine (M500-50CT TESTOMETRIC). The compressive strength for normal bricks 6.865 MPa to 10.298 MPa. The machine was used 100kN load cell. The load was applied to the specimen at a stress rate of (0.05 ± 0.01) MPa/s. The compressive strength was refers to the maximum load or force that a glass bricks can withstand before it fails or fractures under compression.

CHAPTER 4

RESULT AND DISCUSSION

4.1 Production of Mould

4.1.1 POP Mould

From Figure 4.1 showed that POP mould 1, which utilized composition from Table 3.2 did not dry at room temperature. This is because the plaster of paris is calcium sulphate hemihydrate. When calcium sulphate hemihydrate connected with water, the hydration and crystallization process was occurred and the material become harden (Geraldo et al., 2018). Due to the weight percentage of plaster of paris in Table 3.2 not being sufficient and lead to the POP mould 1 did not dry within 5 days at room temperature.

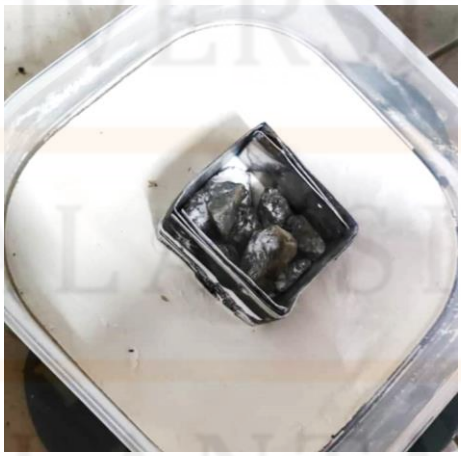

Figure 4.1: The POP mould 1

Apart from that, the POP mould 2 using composition 2 as shown in Figure 4.2 exhibited cracks during drying process at room temperature. The differences between POP mould 2 and POP mould 3 were discarding the river sand and increasing 8% of plaster of paris and 2% of water. Thus, the reason of the failure for POP mould 2 was the unsuitable composition and the use of river sand. River sand might contain harmful or unwanted impurities and have different qualities of sand thereby causing the failure of POP mould 2. However, POP mould was not suitable for the firing process due to the presence of oxygen in plaster of paris and its water absorption properties. When plaster of paris undergoes a firing process, the oxygen and water were released. This might occur internal stresses in the plaster of paris, ultimately leading to the generation of stress, and in some cases, resulting in an eventual explosion.

Figure 4.2: The POP mould 2

Figure 4.3: The POP mould 3

4.1.2 Industrial Clay Mould

Figure 4.4 was showed an industrial clay mould was produced by using industrial clay. The industrial clay mould A, B, C was conducted drying process in an oven and a firing process in furnace. Figure 4.5 was presented the industrial clay mould was dried using oven and Figure 4.6 was presented the industrial clay mould was fired using furnace.

Figure 4.4: The industrial clay mould before oven

Figure 4.5: The industrial clay mould after oven

Figure 4.6: The industrial clay mould after furnace

Table 4.1: The weight of the industrial clay mould before, after oven and after firing

Mould	Before Oven(g)	After Oven(g)	After firing(g)
A	527.5	398 .5	361.0
B	404.0	332.5	298.0
C	453.0	369.5	329.0

Based on Table 4.1, the drying shrinkage process was occurred in the oven during the drying process because the loss of water layers. The weights of mould A, B and C decreased from 527.5g to 398.5g, 404g to 332.5g and 453g to 369.5g, respectively. The vitrification process of the industrial clay mould was occurred in the

furnace during the firing process, resulting the industrial clay mould became hard (Wattanasiriwech et al., 2009). The weight of the industrial clay mould A, B, C was decreased because of the firing shrinkage. The weight of the mould A was decreased from 398.5g to 361g, mould B was decreased from 332.5g to 298g and mould C was decreased from 369.5g to 329g after the firing process. However, during the second production of the industrial clay mould by using industrial clay, it had scattered into small pieces. The colour changes process was occurred after the drying process and after the firing process. The colour of the industrial clay mould was changed from dark brown to light brown during the dying process. During the firing process, the light brown was changed to red. Hence, Figure 4.6 was showed the industrial clay contains iron oxides because the industrial clay mould turned red after the firing process (Valanciene et al., 2010).

4.1.3 Clay Mix Mould

The production of clay mix mould was used the composition of ball clay, kaolin and sawdust in Table 3.5. Figure 4.7 was showed the clay mix mould crack during drying at room temperature. This is because the aluminium plate was absorbed the energy and transferred energy to the mould and lead to the mould conduct the thermal shock. Besides that, the drying shrinkage decreased the weight of the mould and the size of the mould became small. Due to the aluminium plate was stronger than mixture of clay mix, thus during the drying shrinkage the clay mix mould can't shrinkage and lead to the mould cracks.

Figure 4.7: The clay mix mould production with aluminium plate

Hence, the second time for production of clay mix mould was carried out without an aluminium plate. Figure 4.8 showed that the clay mix mould didn't crack and it remained in good condition during the drying process at room temperature.

Figure 4.8: The clay mix mould production without aluminium plate

Based on Table 4.2, the 5 clay mix mould with same composition (CMM 1, CMM 2, CMM 3, CMM 4, CMM 5) was conducted the drying shrinkage and the firing shrinkage. During the drying process in oven, the weight of clay mix moulds was decreased because of the water layer was evaporated. The weight of CMM1 was

decreased from 114.5g to 87.5g, the weight of CMM2 was decreased from 106.5g to 83.5g, the weight of CMM3 was decreased from 106g to 83.5g, the weight of CMM4 was decreased from 74.5g to 61g and CMM5 decreased from 79.5 to 65g. After the drying process, the clay mix mould was conducted the firing process to remove the interior water of the mould and the vitrification process was occurred (Wattanasiriwech et al., 2009). After the firing process, the weight of CMM1, CMM2, CMM3, CMM4, CMM5 were decreased from 87.5g to 74g, 83.5g to 71.5g, 83.5g to 71g, 61g to 52g and 65g to 55.5g. The colour was changed during the drying and firing process. First, the colour of clay mix mould before oven was presented grey colour in Figure 4.8 and after conducted the drying process in oven turned to white grey in Figure 4.9. After conducted the firing and vitrification process, the colour of clay mix mould was turned into white colour in Figure 4.10. Due to the main composition of the clay mix mould was ball clay. Ball clay was showed light or near white colour after being fired (Zaid et al., 2017).

Table 4.2: The weight of clay mix mould before, after oven and after firing

Clay Mix Mould	Before Oven(g)	After Oven(g)	After Firing(g)
CMM1	114.5	87.5	74.0
CMM2	106.5	83.5	71.5
CMM3	106.0	83.5	71.0
CMM4	74.5	61.0	52.0
CMM5	79.5	65.0	55.5

Figure 4.9: The clay mix mould after undergo drying process in oven

Figure 4.10: The clay mix mould after undergo firing process in furnace

4.2 Thermogravimetric Analysis (TGA)

Based on Figure 4.11, the TG curve was obtained using heating a rate 10℃/min. The mass loss (%) of the POP mould was observed between 30℃ to 80℃ because the pre-dehydroxylation was occurred and the water propagation. The weight loss (%) during pre-dehydroxylation was 0.2%. On the other hand, the dehydroxylation was observed from 450℃ to 690℃ and the weight loss of POP mould was 1.33%. The chemical reaction for the dehydroxylation of the POP mould was $CaSO_4 \cdot 2H_2O \rightarrow CaSO_4$ (Saukani et al., 2019).

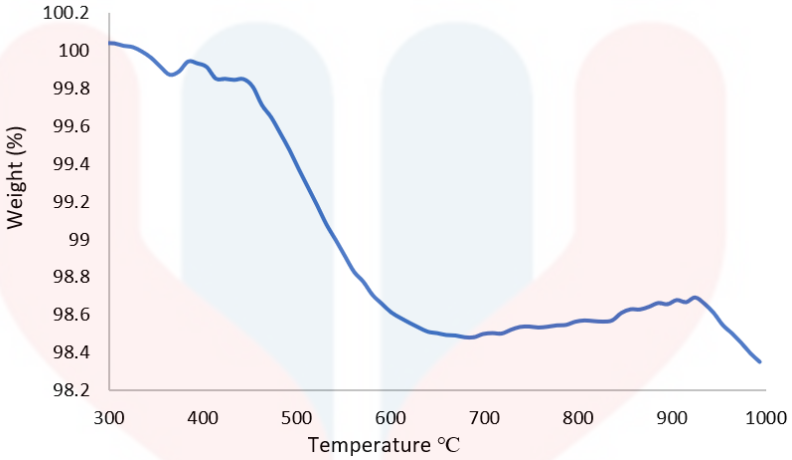

Figure 4.11: TGA curve of POP mould

Furthermore, the degradation process of the industrial clay mould was occurred during the temperature between 230℃ to 550℃ and the weight loss of the industrial clay mould was 6.9% in Figure 4.12. The degradation temperatures of the samples closely align with the phase transformation from crystalline clay particles to amorphous heated clay, indicating a narrow temperature range for this transition. The chemical equation:

$$2Al_2Si_2O_5(OH)_4 \rightarrow 2Al_2Si_2O_7 + 4H_2O$$

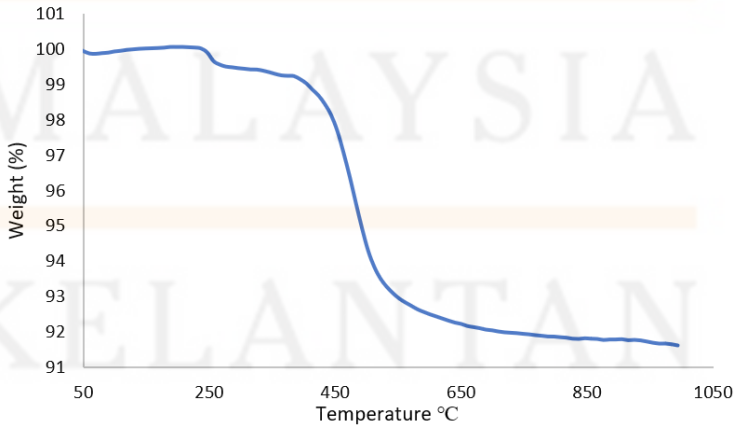

Figure 4.12: TGA curve of Industrial clay mould

The observed endothermic peak in the industrial clay mould was the result of water being released from the clay's structural and coordinated water molecules through their dehydroxylation. Hence, 93.1% of the industrial clay mould was left-undecomposed and the industrial clay mould was thermally stable at high temperature (Malu et al., 2018).

Figure 4.13 was showed TGA curved of the clay mix mould. The TGA curve was illustrated the weight loss (%) in the temperature range 247℃ to 267℃. The weight loss (%) was occurred around 0.7% because of the dehydration process. Next, the second stage of major weight loss (%) happened at temperatures between 450℃ and 550℃, where the TG curve displays a weight loss of 8%. This stage was represented the dehydroxylation process and the loss of structural water (Abd Aziz et al., 2019).

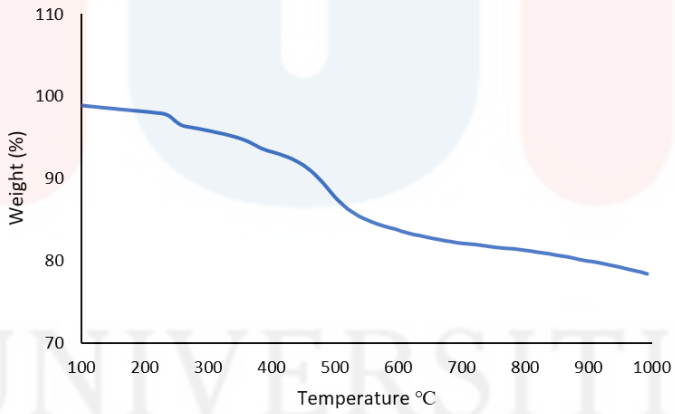

Figure 4.13: TGA curve of clay mix mould

4.3 X-Ray Diffraction (XRD)

The machine used for XRD analysis was Bruker D2 Phaser and diffrac.eva was employed to analyse the data. Figure 4.14 was showed the XRD pattern for waste glass powder. From the XRD analysis, the waste glass was exhibited low crystallinity with 100% amorphous distribution. Additionally, the waste glass was represented a general

amorphous band between 20º and 30º 2(θ), which means the existence of high value of silica with non-crystalline phase (Hasan et al., 2021).

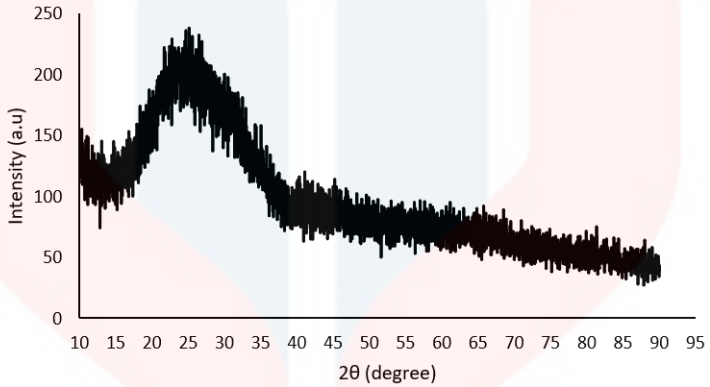

Figure 4.14: The XRD pattern of waste glass

Figure 4.15 showed the XRD patter of industrial clay. The industrial clay showed distribution of crystalline peak. The crystallinity of industrial clay was 62.2%. Besides that, the main materials of industrial clay were kaolinite (COD 1541965), quartz (COD 9011493) and berlinite (COD 9006552). The peak of kaolinite found was at 2θ = 12.3º, 20.7º, 24.8º, 27.3º, 34.9º 38.5º and 62.1º corresponding with analysis obtained by previous study (Kłosek-Wawrzyn et al., 2013). Next, the peak of quartz was founded at 2θ = 20.9º, 26.6º, 55.1º, 59.8º and 68º (Wattanasiriwech et al., 2009).

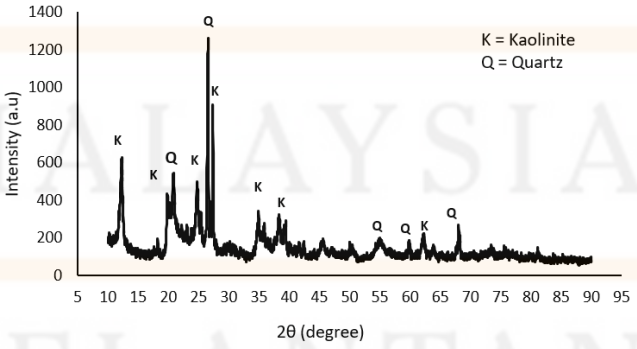

Figure 4.15: The XRD pattern of industrial clay

4.4 Visual Inspection

Figure 4.16 was showed the production of glass bricks by using cullet of waste glass with firing temperature 850 ℃ and 8 hours exposure time. The samples were clearly showed the cullet of waste glass not totally melted but adhered together for the outer layer of glass bricks because the cullet of waste glass started adhesive and soften when the temperature reach 700 ℃ (Shelby, 2020). The cullet of waste glass was undergoing the adhesion process and stick together outer layer of the glass bricks. Figure 4.17 showed the production of glass bricks by using the cullet of waste glass with the firing temperature 950 ℃ and 8 hours exposure time. The samples were observed the glaze and the reflection of glass bricks. After that, the cullet of waste glass was melted and adhesive together in Figure 4.16. Figure 4.18 showed the visual inspection comparison between 2 firing temperature 850 ℃ and 950 ℃ for production glass bricks. The surface of glass bricks with firing temperature 850 ℃ was roughly and the surface of glass bricks with the firing temperature 950 ℃ was smoother. Apart from that, Figure 4.18 showed the side view of glass bricks between 2 firing temperature 850 ℃ and 950 ℃ for the production of glass bricks. In Figure 4.18, the difference in the melting stage is evident when 850 ℃ and 950 ℃ were used for the firing process. The outer layer of glass bricks with 850 ℃ show the original shape of cullet waste glass.

Figure 4.16: The production of glass bricks by using cullet of waste glass with firing temperature 850 ℃ and 8 hours exposure time

Figure 4.17: The production of glass bricks by using cullet of waste glass with 950 ℃ and 8 hours exposure time

a)

b)

Figure 4.18: The side view comparison between 2 firing temperature (a) 850 ℃ and (b) 950 ℃ for production of glass bricks

4.5 True Density and Apparent Porosity

Based on Figure 4.19, the result showed the true density of 850 glass bricks was lower than 950 glass bricks. The true density of 850 glass bricks was 2.479 g/cm^3. The true density of 950 glass bricks was 2.482 g/cm^3. The firing process of 950 glass bricks

which was using 950 ℃ with 8 hours exposure time shows the good density than using 850 ℃. The firing temperature was extremely important role to determine the true density of glass bricks. The firing process with low temperature was showed low true density. In contrast, the firing process with high temperature was showed high true density. Generally, the true density of normal brick was around 1.8 to 2.0 g/cm^3 (Chiang et al., 2008). Thus, 950 glass bricks was showed the better adhesive particle.

On the other hands, Figure 4.20 was showed the apparent porosity of two glass bricks by using 2 different firing temperature. The apparent porosity of 850 glass bricks was presented 0.707% and the apparent porosity of 950 glass bricks was 0.513%. The percentage of apparent porosity of 8508 glass bricks was higher than 950 glass bricks because the cullet of waste glass didn't melt and fuse together.

Apart from that, Figure 4.21 was showed the percentage of water absorption for 8508 glass bricks and 950 glass bricks. The water absorption of the 850 glass bricks was showed 0.285%. Next, the water absorption of 950 glass brick was showed lower with 0.198%. The water absorption of 850 glass bricks was higher because the apparent porosity of 850 glass bricks was higher, leading to the 850 glass bricks absorbing more water.

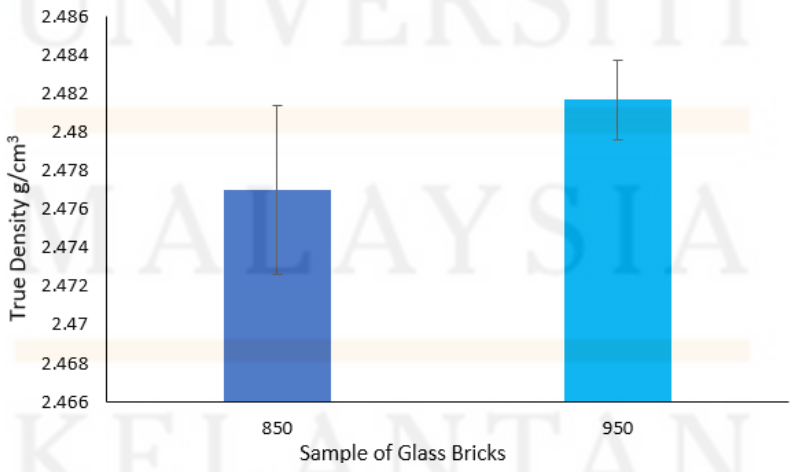

Figure 4.18: The result of true density for two difference firing temperature for production glass bricks

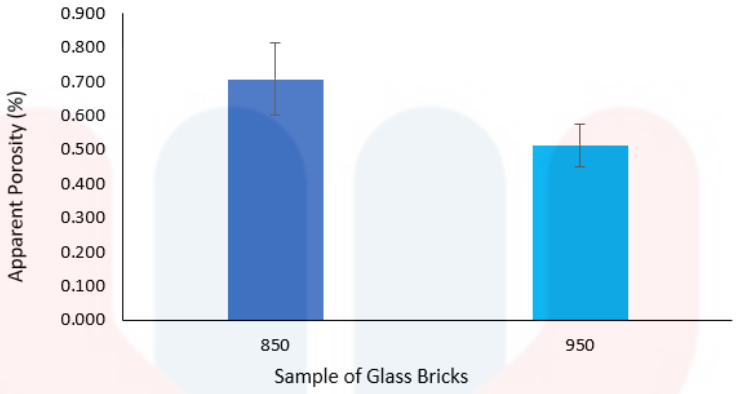

Figure 4.19: The result of apparent porosity for two difference firing temperature for production glass bricks

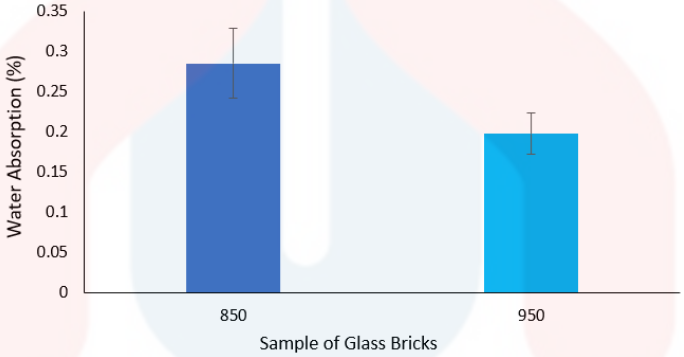

Figure 4.20: The result of water absorption of two difference firing temperature for production glass bricks

4.6 Compressive Strength

Based on Figure 4.22, the compressive strength of 850 glass bricks and 950 glass bricks was shown. The compressive strength of 950 was showed higher compressive strength with 23.452 MPa. The compressive strength of 850 was showed 22.484 MPa. Refer to previous study, higher firing temperature were found to increase the compressive strength of the glass bricks (Brito et al., 2023). According to previous study, compressive strength was decreased with the increase of total porosity (Liu et al.,

2018). In this research, it showed that 850 glass bricks with higher porosity exhibit lower compressive strength compared to 950 glass bricks. 950 was exhibited the better compressive strength.

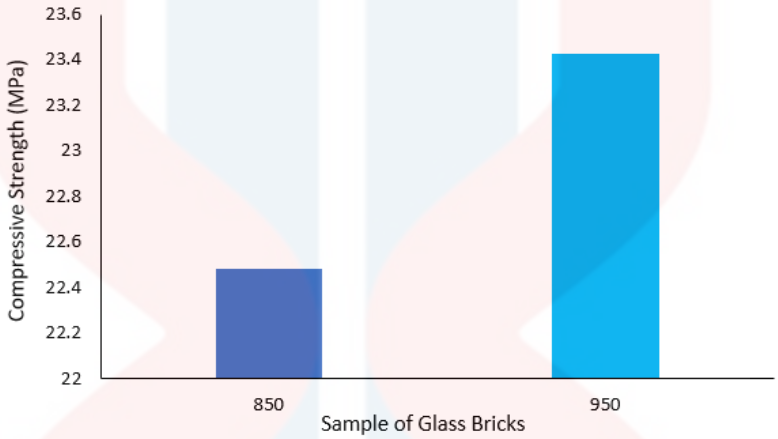

Figure 4.21: Compressive strength of two different firing temperature glass bricks

4.7 Fourier Transform Infrared Spectroscopy (FTIR)

Based on Figure 4.23, the FTIR spectra of waste glass was shown. From figure 4.23 was observed the Si-O-Si bending modes at ≈ 490 cm^{-1} wavenumbers. A small peak at ≈ 780 cm^{-1} was occurred because the Si-O-Si symmetric stretching of bridging oxygens between the silica tetrahedra. After that, Si-O-Si asymmetric stretching was occurred during the peak at ≈ 1000 cm^{-1} (El-Batal et al., 2010).

After that, Figure 4.24 was showed the FTIR spectra of 850 glass bricks. The Si-O-Si bending vibration at during ≈ 457 cm^{-1} wavenumber. The Si-O stretching mode of non-bridging oxygen was observed during ≈ 960 cm^{-1} and the Si-O-Si antisymmetric stretching of bridging oxygens within the tetrahedra during ≈ 1015 cm^{-1} (El-Batal et al., 2010).

In addition, Figure 4.25 was presented the FTIR spectra of 950 glass bricks. During ≈ 475 cm^{-1} wavenumber, the Si-O-Si bending vibration was occurred and the Si-O stretching mode of non-bridging oxygen was observed at ≈ 970 cm^{-1} in figure 4.25. The Si-O-Si asymmetric stretching was occurred at ≈ 1053 cm^{-1} wavenumber.

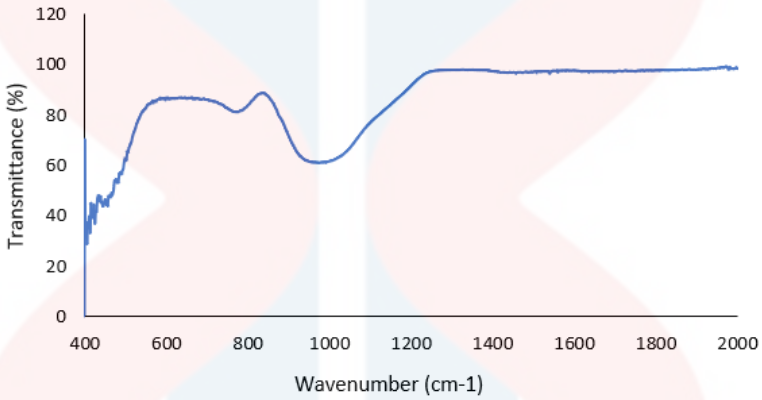

Figure 4.22: FTIR spectra of waste glass

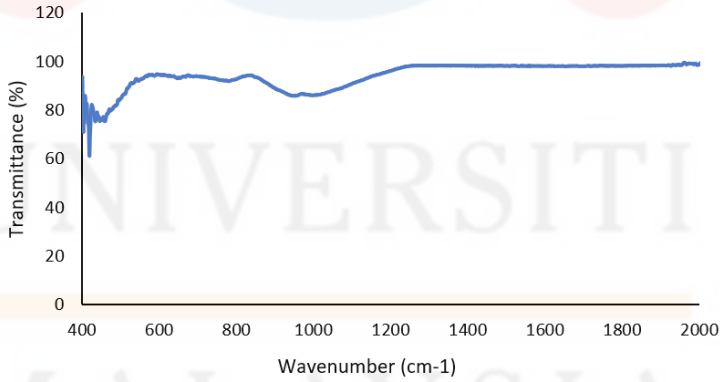

Figure 4.23: FTIR spectra of 850 glass bricks

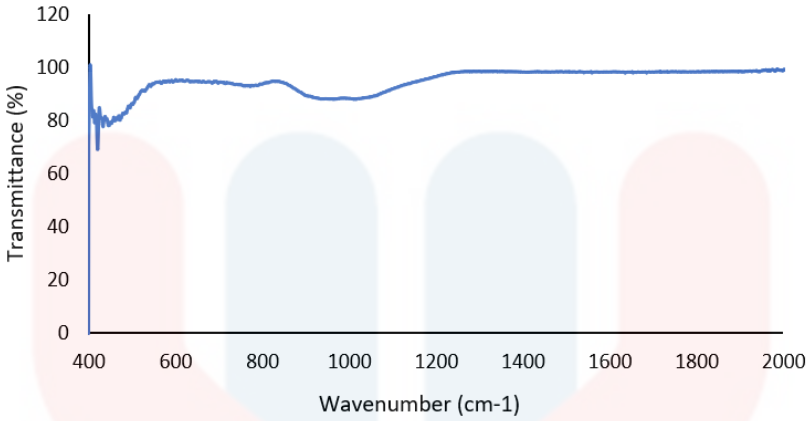

Figure 4.24: FTIR of 950 glass bricks

CHAPTER 5

CONCLUSION AND RECOMMENDATIONS

5.1 Conclusion

In this study, the properties of glass bricks by using cullet of waste glass and different firing temperature were analysed. The effect of different firing temperature of glass bricks toward the physical and structure properties of glass bricks was identified. It can be concluded that the glass bricks with higher firing temperature can improve the properties of glass bricks. Thus, the glass bricks with higher firing temperature have high true density, high compressive strength low water absorption and low apparent porosity. However, the glass bricks with lower firing temperature have low true density, compressive strength, high water absorption and apparent porosity. In conclusion, firing temperature was extremely significant for production of glass bricks by using waste glass.

5.2 Recommendation

Since the higher firing temperature used in this study was only 950℃, the cullet of waste glass does not enough temperature for them to adhesive nicely. The properties of glass bricks will improve with increase the firing temperature. Thus, the recommendation to enhance the study result is increasing the firing temperature. For example, 1000 ℃, 1100 ℃ and 1200 ℃.

Besides that, the surface morphology of glass bricks can observe by using Scanning Electron Microscope (SEM). SEM can capture high-resolution images of the glass bricks surface because SEM have a high magnification up to 30000X. SEM can used to observe the grain structure, grain boundaries, and pore structure of the sample. Thus, SEM can used to observe the porosity of glass bricks.

REFERENCES

Abd Aziz, M. H., Othman, M. H. D., Hashim, N. A., Adam, M. R., & Mustafa, A. (2019). Fabrication and characterization of mullite ceramic hollow fiber membrane from natural occurring ball clay. *Applied Clay Science*, *177*, 51-62.

Achintha, M. (2016). Sustainability of Glass in Construction. In *Sustainability of Construction Materials* (pp. 79-104). Elsevier.

Aktas, B., Albaskar, M., Yalcin, S., & Dogru, K. (2016). Optical properties of soda-lime-silica glasses doped with peanut shell powder. *Archives of Materials Science and Engineering*, *82*(2), 57--61.

Alabduljabbar, H., Benjeddou, O., Soussi, C., Khadimallah, M. A., & Alyousef, R. (2021). Effects of incorporating wood sawdust on the firing program and the physical and mechanical properties of fired clay bricks. *Journal of Building Engineering*, *35*, 102106.

Álvarez, M., Ferrández, D., Morón, C., & Atanes-Sánchez, E. (2021). Characterization of a new lightened gypsum-based material reinforced with fibers. *Materials*, *14*(5), 1203.

Aubert, J.-E., Maillard, P., Morel, J.-C., & Al Rafii, M. (2016). Towards a Simple Compressive Strength Test for Earth Bricks? *Materials and Structures*, *49*, 1641-1654.

Brito, L. B. Q., Agrawal, P., De Mélo, T. J. A., De Figueiredo Brito, G., & Da Silva Morais, C. R. (2023). Recycling of Waste Glass for the Production of Hollow Blocks Using the Kiln-Casting Process. *Cleaner Waste Systems*, 100079.

Chen, G., Lee, H., Young, K. L., Yue, P. L., Wong, A., Tao, T., & Choi, K. K. (2002). Glass Recycling in Cement Production—An Innovative Approach. *Waste Management*, *22*(7), 747-753.

Chiang, K.-Y., Chien, K.-L., & Hwang, S.-J. (2008). Study on the characteristics of building bricks produced from reservoir sediment. *Journal of Hazardous Materials*, *159*(2-3), 499-504.

de Moraes, F., Müller, W., Frischat, G. H., & Müller, R. (2008). Corrosion and crystallization at the inner surfaces of glass bricks. *Journal of Non-Crystalline Solids*, *354*(2-9), 284-289.

Demir, I. (2009). Reuse of Waste Glass in Building Brick Production. *Waste management & research*, *27*(6), 572-577.

El-Batal, F., Khalil, E., Hamdy, Y., Zidan, H., Aziz, M., & Abdelghany, A. (2010). FTIR spectral analysis of corrosion mechanisms in soda lime silica glasses doped with transition metal oxides. *Silicon*, *2*, 41-47.

Epp, J. (2016). X-Ray Diffraction (XRD) Techniques for Materials Characterization. In *Materials Characterization Using Nondestructive Evaluation (NDE) Methods* (pp. 81-124). Elsevier.

Geraldo, R. H., Souza, J. D., Campos, S. C., Fernandes, L. F., & Camarini, G. (2018). Pressured recycled gypsum plaster and wastes: Characteristics of eco-friendly building components. *Construction and Building Materials*, *191*, 136-144.

Hamidon, A., Badarulzaman, N. A., & Muhamad Nor, M. A. A. (2015). Recycled Glass Potential as Porous Ceramic Determine by Spectroscopy Analysis. Advanced Materials Research,

Hasan, M. R., Siddika, A., Akanda, M. P. A., & Islam, M. R. (2021). Effects of Waste Glass Addition on The Physical and Mechanical Properties of Brick. *Innovative Infrastructure Solutions*, *6*, 1-13.

Hasanuzzaman, M., Rafferty, A., Sajjia, M., & Olabi, A.-G. (2016). Properties of glass materials. https://doi.org/10.1016/B978-0-12-803581-8.03998-9

Islam, M. S., Sharmin, N., Moniruzzaman, M., & Akhtar, U. S. (2016). Effect of soda lime silica glass waste on the basic properties of clay aggregate. *Int. J. Sci. Eng. Res*, *7*(4), 149-153.

Kłosek-Wawrzyn, E., Małolepszy, J., & Murzyn, P. (2013). Sintering behavior of kaolin with calcite. *Procedia Engineering*, *57*, 572-582.

Liu, H., Luo, G., Wei, H., & Yu, H. (2018). Strength, permeability, and freeze-thaw durability of pervious concrete with different aggregate sizes, porosities, and water-binder ratios. *Applied Sciences*, *8*(8), 1217.

Malu, S., Ugye, J., & Donatus, R. (2018). Characterization of clay for industrial application by physicochemical, XRF, and TGA methods. *FUW Trends in Science & Technology Journal*, *3*(1), 314-318.

Mehta, A., & Ashish, D. K. (2020). Silica Fume and Waste Glass in Cement Concrete Production: A Review. *Journal of Building Engineering*, *29*, 100888.

Rangga, J. U., Ismail, S. N. S., Rasdi, I., & Karuppiah, K. (2022). Waste Management Costs Reduction and the Recycling Profit Estimation from the Segregation Programme in Malaysia. *Pertanika Journal of Science & Technology*, *30*(2).

Saadatkhah, N., Carillo Garcia, A., Ackermann, S., Leclerc, P., Latifi, M., Samih, S., Patience, G. S., & Chaouki, J. (2020). Experimental methods in chemical engineering: Thermogravimetric analysis—TGA. *The Canadian Journal of Chemical Engineering*, *98*(1), 34-43.

Saukani, M., Arief, S., Syahrillah, G., & Hidayat, N. (2019). The low concentration of sodium hydroxide influence on the compressive strength of fly ash/natural kaolin-based geopolymer. IOP Conference Series: Materials Science and Engineering,

Shelby, J. E. (2020). *Introduction to Glass Science and Technology*. Royal Society of Chemistry.

Stryszewska, T., & Kańka, S. (2019). Forms of Damage of Bricks Subjected to Cyclic Freezing and Thawing in Actual Conditions. *Materials*, *12*(7), 1165.

Valanciene, V., Siauciunas, R., & Baltusnikaite, J. (2010). The influence of mineralogical composition on the colour of clay body. *Journal of the European Ceramic Society*, *30*(7), 1609-1617.

Wattanasiriwech, D., Srijan, K., & Wattanasiriwech, S. (2009). Vitrification of illitic clay from Malaysia. *Applied Clay Science*, *43*(1), 57-62.

Zaid, S. N. A., Morad, N. A. A. J., Abdullah, M. A. A., & Nor, M. A. A. M. (2017). Preliminary study on chemical and physical properties of ball clay and its sintered ceramic pieces from Kampung Dengir, Besut, Terengganu. *Journal of Sustainability Science and Management Special Issue*.

Zhang, Z., Wong, Y. C., Arulrajah, A., & Horpibulsuk, S. (2018). A review of studies on bricks using alternative materials and approaches. *Construction and Building Materials*, *188*, 1101-1118.

Zheng, J., Xu, K., Wang, H., Sun, W., Sun, J., & Liu, J. (2023). Effect of Bentonite Content on the Suspension Stability of a Glaze Slurry and Final Enamel Performance. *Ceramics International*, *49*(6), 9493-9501.

APPENDIX A

Pattern: COD 1541965 Radiation: 1.54060 Quality: Quality Unknown

Formula	Al2H4O9Si2
Name	
Name (mineral)	
Name (common)	
Status	Status Unknown
Ambient	Yes

Lattice:	Triclinic
S.G.:	C 1 (1)

a =	5.14000
b =	8.93000
c =	7.37000
a/b =	0.57559
c/b =	0.82531

alpha =	91.800
beta =	104.500
gamma =	90.000
Z =	2

Mol. weight =	
Volume [CD] =	327.34
Dx =	
Dm =	
I/Icor =	1.190

Primary Reference
Drits V.A., Kashaev A.A., "An x-ray study of a single crystal of kaolinite", Kristallografiya 5 (1960) 224-227.

Wavelength:	1.54060
Filter:	Not specified
d-spacing:	

d	2θ	I fix	h	k	l	d	2θ	I fix	h	k	l
7.13150	12.402	999	0	0	1	2.24300	40.171	28	1	3	-2
4.46260	19.879	177	0	2	0	2.22170	40.573	7	2	2	-1
4.36140	20.346	469	1	-1	0	2.21540	40.694	2	-2	2	1
4.33130	20.489	13	1	1	0	2.18850	41.216	32	-1	3	2
4.15840	21.350	440	1	1	-1	2.18510	41.284	30	2	0	1
4.11220	21.593	235	-1	1	1	2.18070	41.371	11	2	-2	0
3.83940	23.148	309	0	2	-1	2.16570	41.670	3	2	2	0
3.72900	23.843	124	0	2	1	2.14950	41.999	2	0	4	-1
3.56570	24.952	616	0	0	2	2.12690	42.467	28	0	-2	3
3.42330	26.008	14	1	-1	1	2.11010	42.822	8	0	4	1
3.36900	26.434	185	1	1	1	2.07040	43.685	2	0	2	3
3.13610	28.437	42	1	1	-2	2.05610	44.004	8	-2	2	2
3.08570	28.912	33	-1	1	2	1.98800	45.595	91	1	-3	2
2.83090	31.579	8	0	2	-2	1.98500	45.668	109	-2	0	3
2.74270	32.622	95	0	2	2	1.97590	45.890	1	2	-2	1
2.56270	34.985	84	-1	3	0	1.94940	46.550	31	2	2	1
2.55680	35.068	73	2	0	-1	1.93360	46.953	79	1	3	2
2.54440	35.245	81	1	3	0	1.92870	47.080	1	1	-1	3
2.52420	35.536	120	1	3	-1	1.91970	47.314	23	0	4	-2
2.52040	35.592	49	1	-1	2	1.90460	47.712	5	1	1	3
2.49320	35.993	127	-1	3	1	1.89020	48.099	33	1	3	-3
2.48810	36.069	135	2	0	0	1.86450	48.805	14	0	4	2
2.48280	36.149	21	1	1	2	1.83790	49.558	43	-1	3	3
2.37720	37.814	81	0	0	3	1.83600	49.613	24	2	0	2
2.33770	38.478	206	-1	3	-1	1.82770	49.853	29	2	2	-3
2.33310	38.557	191	2	0	-2	1.80380	50.560	8	-1	-1	4
2.32590	38.681	18	-1	-1	3	1.79990	50.677	9	-2	2	3
2.29270	39.264	31	-1	1	3	1.78290	51.195	31	0	0	4
2.28630	39.379	239	1	3	1	1.71160	53.493	34	2	-2	2

Pattern: COD 2106432 Radiation: 1.54060 Quality: Quality Unknown

Formula	Al9.1Ca2.4K1.6Mg0.7Na0.9O72Si26.9
Name	
Name (mineral)	
Name (common)	
Status	Status Unknown
Ambient	Yes

Lattice:	Hexagonal
S.G.:	P 63/m m c (194)

a =	13.25200
c =	14.81000
a/b =	1.00000
c/b =	1.11757
Z =	1

Mol. weight =	
Volume [CD] =	2252.42
Dx =	
Dm =	
I/Icor =	5.520

Primary Reference
Schlenker J.L., Pluth J.J., Smith J.V., "Dehydrated natural erionite with stacking faults of the offretite type", Acta Crystallographica B (24,1968-38,1982) 33 (1977) 3265-3268.

Wavelength :	1.54060
Filter:	Not specified
d-spacing:	

d	2θ	I fix	h	k	l	d	2θ	I fix	h	k	l
11.47660	7.697	999	1	0	0	2.67530	33.468	44	4	0	2
9.07160	9.742	311	1	0	1	2.67520	33.469	5	1	3	3
7.40500	11.942	132	0	0	2	2.50440	35.827	39	4	1	0
6.62600	13.352	194	1	1	0	2.48080	36.179	17	2	3	2
6.22220	14.223	45	0	1	2	2.48060	36.182	4	4	0	3
5.73830	15.429	19	2	0	0	2.46930	36.354	2	1	4	1
5.35070	16.554	8	2	0	1	2.46890	36.360	20	2	2	4
4.93780	17.950	9	1	1	2	2.46830	36.369	2	0	0	6
4.53580	19.555	31	2	0	2	2.44610	36.711	1	1	2	5
4.53490	19.559	52	0	1	3	2.37240	37.894	2	1	4	2
4.33770	20.458	91	2	1	0	2.31310	38.904	6	1	1	6
4.16290	21.327	33	1	2	1	2.29530	39.218	4	5	0	0
3.82550	23.233	53	3	0	0	2.26820	39.706	6	5	0	1
3.74280	23.754	91	1	2	2	2.26790	39.712	3	4	0	4
3.74230	23.757	3	0	2	3	2.23340	40.351	5	1	4	3
3.70250	24.016	9	0	0	4	2.20870	40.823	5	3	3	0
3.52370	25.254	123	0	1	4	2.19240	41.140	8	5	0	2
3.39880	26.199	13	3	0	2	2.14530	42.085	2	1	2	6
3.31300	26.890	29	2	2	0	2.11650	42.686	21	3	3	2
3.25850	27.348	8	1	2	3	2.08140	43.442	4	2	4	2
3.23210	27.576	18	1	1	4	2.08130	43.444	4	5	0	3
3.18300	28.010	5	3	1	0	2.08070	43.457	4	0	1	7
3.11200	28.662	7	1	3	1	2.07440	43.596	3	1	4	4
3.11110	28.671	53	0	2	4	2.07410	43.603	2	0	3	6
2.92430	30.545	4	1	3	2	1.98580	45.648	8	1	5	2
2.86910	31.148	61	4	0	0	1.96790	46.087	2	2	3	5
2.86800	31.160	12	0	1	5	1.95080	46.515	7	5	0	4
2.81680	31.741	64	4	0	1	1.91240	47.506	5	1	4	5
2.81610	31.749	84	1	2	4	1.87160	48.607	6	3	4	1

APPENDIX B

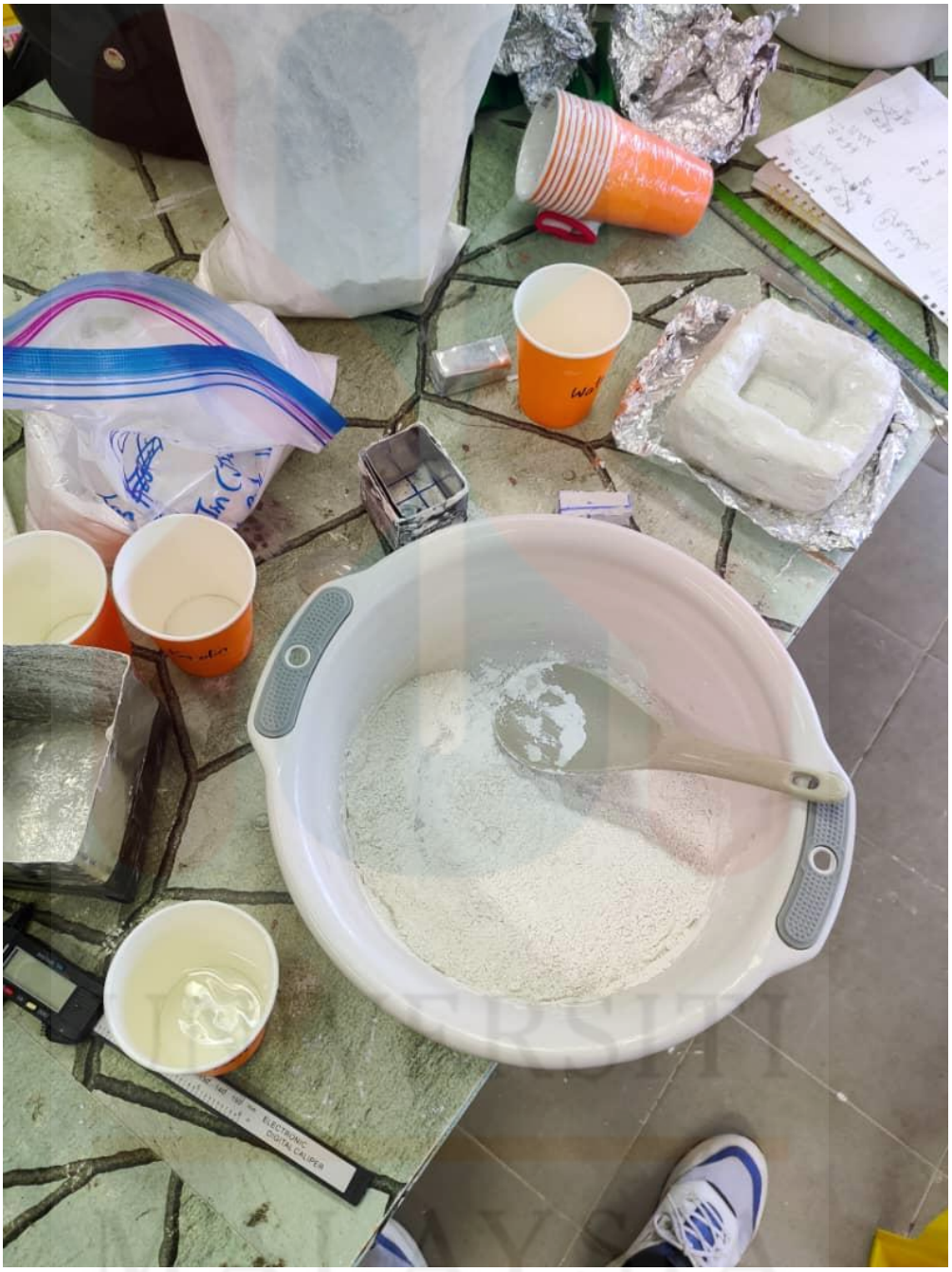

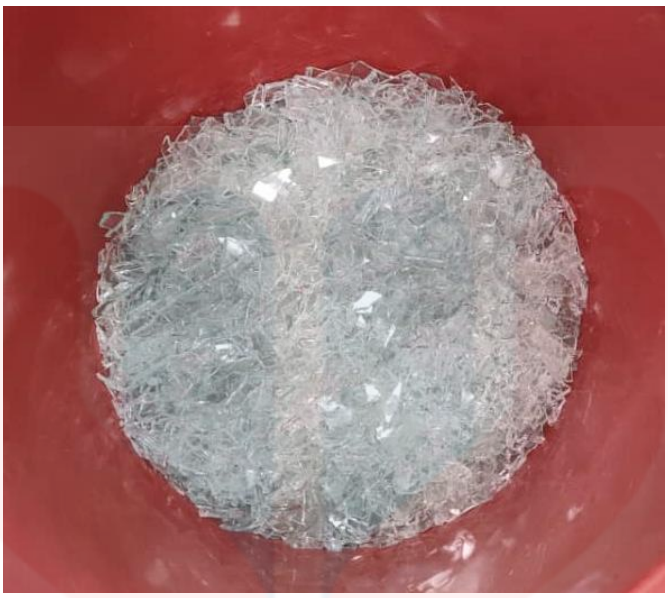

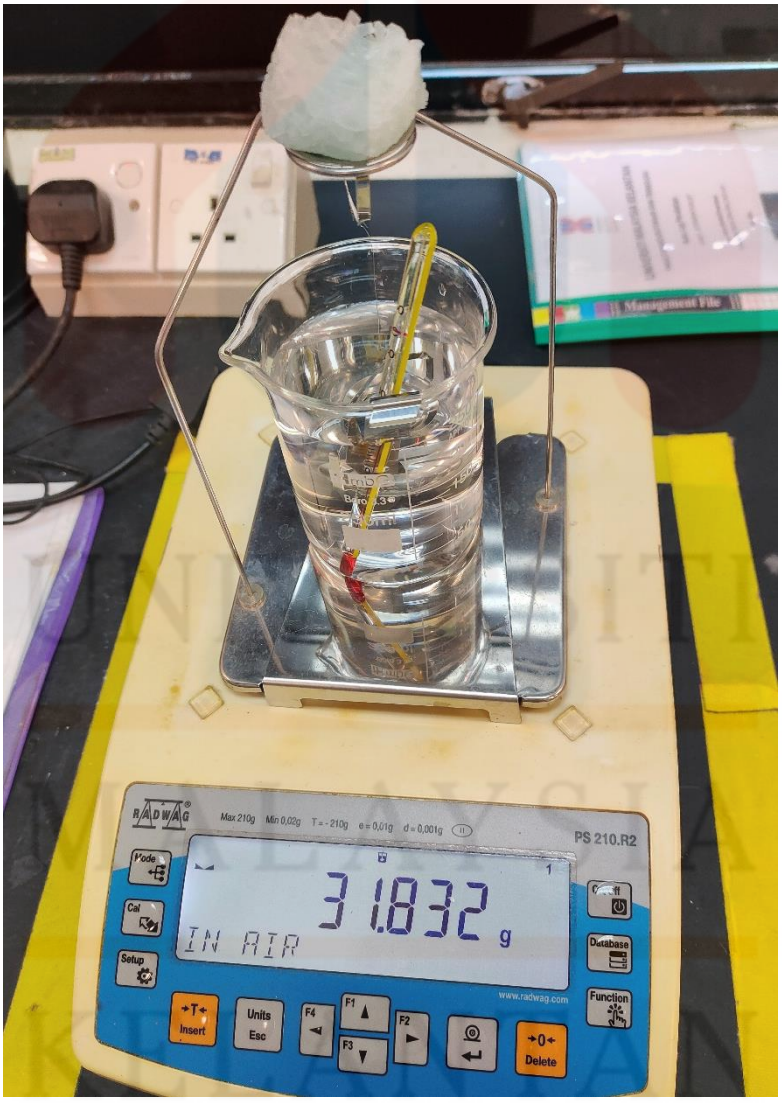
RADWAG
PS 210.R2
31.832 g
IN AIR
Units
Esc
Insert
Delete
Function
Database
Setup
Cal
Mode

APPENDIX C

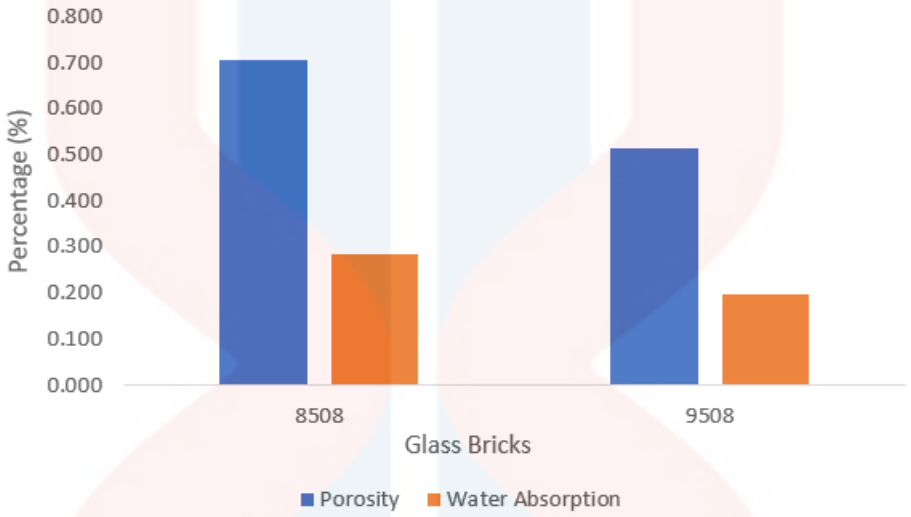

Figure: The relationship between porosity and water absorption